

# Spectroscopic Studies of Arrays of Multiwalled Carbon Nanotubes

Brian Kimball<sup>a</sup>, Joel B. Carlson<sup>a</sup>, Asher Pembroke<sup>a</sup>, Krzysztof Kempa<sup>b</sup>, Z. F. Ren<sup>b</sup>, Pengfei Wu<sup>c</sup>, Chandra Yelleswarapu<sup>c</sup>, Thomas Kempa<sup>b</sup>, Glynda Benham<sup>d</sup>, Y. Wang<sup>b</sup>, A. Herczynski<sup>b</sup>, Jakub Rybczynski<sup>b</sup>, Z. P. Huang<sup>e</sup>, and D.V.G.L.N. Rao<sup>c</sup>

<sup>a</sup>U.S. Army, Natick Soldier Center, Natick, MA 01760

<sup>b</sup>Boston College, Physics Department, Chestnut Hill, MA 02467

<sup>c</sup>University of Massachusetts Boston, Physics Department, Boston, MA 02125

<sup>d</sup>MegaWave Corporation, Boylston MA 01505

<sup>e</sup>NanoLab, Inc., Newton, MA 02458

## ABSTRACT

Spectroscopic observations are presented for carbon nanotubes grown on silicon and quartz substrates in a hexagonal honeycomb configuration using self-assembly nanosphere lithography and plasma enhanced chemical vapor deposition method. A white light source is used as an incident beam and light reflected from the surface of the carbon nanotubes results in a distinctive signature in the reflected spectrum. A comparison of non-periodic arrays and periodic arrays of carbon nanotubes show that the reflectance signature is only observed when the carbon nanotubes are oriented in a periodic array. Further observations regarding the light antenna effect observed in nonperiodic arrays are also reported. Theoretical curves show good agreement to experimentally observed phenomena. The unique optical properties of the arrays combined with the excellent mechanical and electrical properties of carbon nanotubes indicate that these materials may find many uses in the field of optoelectronics.

**Key Words:** Band-gap, carbon nanotubes, periodic honeycomb arrays, reflectance data, polarization effects, self-assembly nanosphere lithography, light antenna, dipole antenna

## 1. INTRODUCTION

Conceptually, our interest in the optical properties of carbon nanotubes is based on the work of Edwin Land; specifically with regards to his work in the development of *H-sheet* polarizers. These polarizers are essentially an organic version of the wire grid polarizer<sup>1</sup>. The sheets are comprised of long chain, polymer, polyvinyl alcohol molecules that have been stretched in one dimension. This causes the polymer chains to align along that direction. The polymer can then be doped with an electron rich substance such as iodine. Electrons are free to move up and down the polymer chains. When light is incident on such a material, the electric field component that is parallel to the aligned polymer chains sets the electrons in oscillation along the chain. This effectively absorbs that component of light, thus causing a polarized beam of light to exit the material.

Here, it was reasoned that carbon nanotubes, being quasi one-dimensional metallic structures, should interact with light in a similar way. This should be especially true for aligned carbon nanotubes arrays. At the very least, one would expect to observe interesting polarization effects from aligned CNT arrays. The nanotube arrays are grown on surfaces creating essentially a three dimensional material. Thus we have more flexibility in adjusting the angle of incidence through 90 degrees than is possible with a sheet polarizer, and it is reasonable to expect higher order response as the incident light "sees" a geometry that changes with angle of incidence.

The fact that the nanotubes can be grown to lengths on the order of a wavelength of light hints at the possibility of a strong interaction with light of a similar wavelength. Considering that light is periodic, one would also expect an even stronger interaction with periodic arrays when the array spacing is on the order of a wavelength of light. For very long

polymer chains, as is the case with Land's polarizer sheet, we would not reasonably expect unusual observations as we vary our angle of incidence. We have found, however, that for finite-length, multiwalled carbon nanotubes (MWCNTs), the response is angle dependent. This is understandable if one imagines that the CNTs behave like tiny aerials, or light antennas, which can couple very strongly with incident electromagnetic radiation when certain geometric conditions are met.

We began our evaluations by studying diffraction effects observed from MWCNT arrays. These studies revealed a complex response that could not be described solely in terms of Bragg diffraction. It became clear early on that some aspect of the optical response was due to the geometry of the individual scatters and some portion of the response was due to a collective response determined by the array geometry, such as spacing and CNT configuration. This was first made evident to us through the evaluation of a series of periodic MWCNT arrays of identical spacing, but with varying nanotube height. The characteristic Bragg curves were identical for each sample, but the peak diffraction efficiency was observed to occur at a different wavelength for each sample. This was attributed to a resonant interaction between the incident light and the individual CNT scatterer that occurred within a specific geometry. It was proposed that the individual CNT scatterers were interacting with light in a similar fashion to the way in which radio waves interact with radio antennas.

This observation led to a rather exhaustive series of trials where CNT samples were fabricated with specific geometries to meet some predetermined conditions that were theorized to produce a specific optical signature, that would, in turn, prove out the hypothesis that the nanotubes were indeed behaving like light antennas. These trials proved fruitless because there were simply too many optical phenomena being simultaneously observed. Nevertheless, we have thoroughly documented these phenomena and have concluded that the various observations can be attributed to a number of processes including Bragg diffraction, coherent backscattering, plasmonic resonance and possibly, photonic bandgap behavior (Figure 1).

In order to demonstrate the antenna effect, it was necessary to eliminate the Bragg diffraction and other optical responses associated with the periodicity of the samples. For this purpose, non-periodic arrays of multiwalled CNTs were fabricated where nanotube lengths ranged roughly from  $\lambda/2$  to  $\lambda$  (Figure 2). We observed strong colors reflected from the sample when it was illuminated with white light. We performed spectroscopic studies on the samples at specific locations and also measured the nanotube length at the specific locations. These data were plotted against both theoretical and modeled curves based on antenna theory that relates antenna (CNT) length to

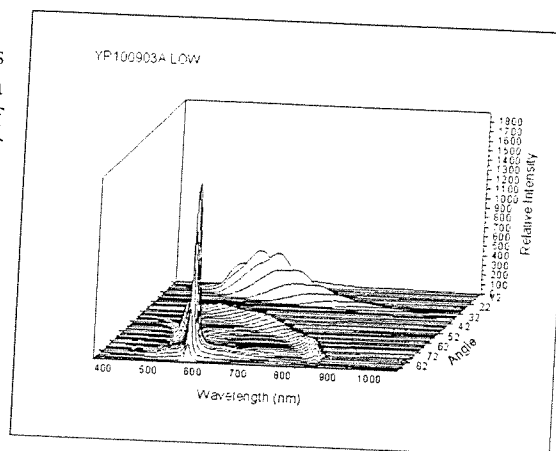


Figure 1. The relative intensity was plotted for variations in the angle as a function of the wavelength for a diffracted beam from a periodic MWCNT array reveals complex interaction with visible light. Optical response is related to array spacing and geometry. Numerous optical effects have been observed including, photonic band gap behavior, plasmonic resonance effects, coherent backscattering and polarization dependent diffraction effects as revealed in 3-D diffraction maps.

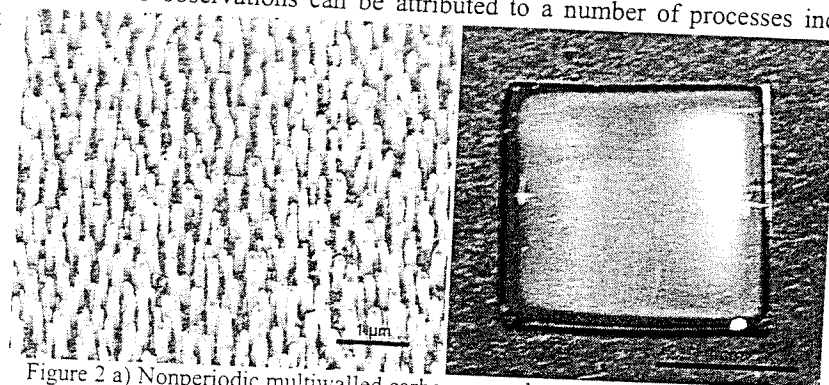


Figure 2 a) Nonperiodic multiwalled carbon nanotube array grown on Si substrate using Ni catalyst and plasma enhanced chemical vapor deposition method. b) Array interacts with light analogous to the way in which radio waves interact with a radio antenna in terms of incident polarization and CNT (antenna) length. Colors are due to resonant interaction of white light with nanotubes of varying length. CNT length decreases left to right.

resonant response<sup>2</sup>. The experimental data matched very well with the predicted response. We also showed that the polarization response of the nonperiodic samples was similar to that which occurs for dipole antennas where the maximum response occurs when the electric field component of the polarized light was parallel to the longitudinal axis of the individual nanotubes and the nanotube length meets the criterion for resonance at a particular wavelength.

In previous studies, periodic arrays of aligned carbon nanotubes were produced using nanosphere self-assembly<sup>3,4</sup>. The arrays were studied for a number of applications including field emitters<sup>5</sup> and nanoelectrodes<sup>6</sup>, components for a micro communications system as well as 2-D photonics crystals. Optical studies were performed detailing the diffraction and polarization properties of periodic CNT arrays<sup>7</sup>. In previous papers we discussed the general optical properties of CNT arrays based on preliminary experimental observations<sup>3,8</sup>. The papers also described the concept of using periodic CNT arrays as 2-D photonic crystals in the visible spectrum. A subsequent paper described the antenna effect observed in nonperiodic arrays of aligned, multiwalled carbon nanotubes as discussed above.<sup>9,10</sup> Previous studies also described nonlinear transmission and scattering in solutions of multiwalled CNTs<sup>11</sup>. Periodic CNT arrays such as these have the potential for numerous applications. The nanotube arrays have unit sizes on the order of a wavelength of visible light and exhibit a strong electromagnetic response. This has allowed for the realization of concepts and devices normally associated with microwaves and radio waves.

In this paper we present some experimental results further documenting the optical properties of aligned, periodic and non-periodic CNT arrays. We present further evidence of the light antenna properties of MWCNTs, and we compare the experimentally observed, optical response to theoretical curves, showing remarkable similarity. We also present data indicating the existence of bandgap behavior based on previous work by another group, who demonstrated bandgap behavior in periodic arrays of metallic rods in the microwave region<sup>12</sup>.

## 2. EXPERIMENTAL AND THEORETICAL EVALUATION

Periodic honeycomb arrays and nonperiodic arrays were evaluated for the way in which they interact with electromagnetic radiation in the visible spectrum. A tungsten lamp was used as a white light source. Continuous wave lasers at 442nm, 532nm and 633nm were used as monochromatic light sources. An Ocean Optics Fiber Optic Spectrometer was used to evaluate scattering from the CNT samples. SEM was used to determine sample geometry.

### 2.1 Sample fabrication

Aligned multi-walled carbon nanotube arrays are fabricated by vapor deposition of a metal catalyst (nickel) on a thermally stable substrate. The coated substrate is exposed to an ammonia/acetylene mixture. The sample is heated to around 600°C. Plasma is induced above the substrate. The plasma induces growth and alignment of the nanotubes. Typical growth time is less than 10 minutes. Arrays grown in this way will generally have too high a concentration of nanotubes for optical studies. They do however make for a highly effective antireflection coating. Less dense arrays can be made by preferentially locating the catalyst to specific locations on the substrate. Non periodic arrays can be made by plasma etching the catalyst coated substrate prior to nanotube growth, thus creating catalyst islands from which a single nanotube can be grown. Periodic arrays can be created using lithographic techniques. E-beam and holographic lithography have been used to create patterned substrates, but the greatest level of success has been achieved using nanosphere self-assembly lithography (Figure 3). This technique utilizes polystyrene nanospheres that are self-assembled on a substrate. Pattern spacing is controlled by nanosphere diameter. The Ni catalyst is deposited over the substrate with the monolayer of nanospheres on the surface. The nanospheres naturally form into a hexagonal formation. The catalyst finds its way to the substrate through the spacing between the nanospheres. The nanospheres

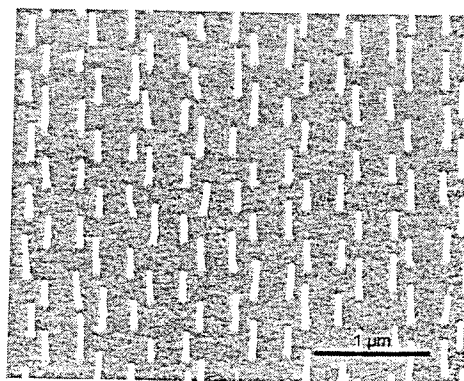


Figure 3. Periodic aligned CNT arrays. Periodic Ni catalyst pattern was created using nanosphere self-assembly lithography.

are then removed, revealing a pattern of triangular islands upon the substrate. Plasma etching is then used to remove the points of the individual triangles effectively leaving a Ni catalyst dot in a honeycomb pattern, from which a single nanotube can be grown. The length of the tubes is determined by the growth time, which is generally on the order of about 10 minutes. Recent improvements in the fabrication process have made it possible to create high quality structures<sup>13</sup>. By optimizing parameters such as heating temperature, deposition thickness of catalytic dots, plasma current intensity and pre-growth plasma etching time, it is possible to improve long range periodicity and uniformity of CNT diameters, straightness and length. Thus it is possible to create nanostructures with varying feature size and spacing that will interact strongly with electromagnetic radiation for wavelengths on the order of the unit size. Figure 3 shows a CNT array created using 590 nm nanospheres.

## 2.2 Antenna effect

We studied the radiation pattern of nonperiodic multi-wall carbon nanotube arrays when scanned with three wavelengths of linearly polarized laser light. Our findings suggest that our samples have many of the properties of a simple phased antenna array of few non-interacting similar elements, emitting one bright main lobe along the angle of incidence and multiple concentric minor lobes. The pattern is steady, symmetric about the array normal, and the minor lobes are visible with the naked eye in dim light.

In general, an array of similar non-interacting sources will interfere with itself independently of the radiation pattern produced by the source elements in the array. For such an array, the full pattern is the product of the normalized contributions from the array factor and the characteristic pattern of the sources. This is the principle of pattern multiplication<sup>14</sup>.

Single antenna patterns are determined by the current distribution in addition to the radiation received from other sources. In general, antennas emit the most radiation in the direction perpendicular to the flow of current, and the intensity at any given angle will depend on the length of the antenna with respect to the excitation frequency. The strongest interaction is for a length equal to one half the wavelength of incident light. For example, the element pattern for a half-wave dipole antenna in terms of the polar angle off axis from the antenna is

$$F_{\text{element}}(\theta) = \cos((\pi/2)\cos(\theta))/\sin(\theta). \quad (1)$$

Essentially, the array factor accounts for the geometrical phase and current phase differences between elements by treating each element as a point source radiating isotropically and allowing their wave fronts to interfere. We show that the angle of beam incidence determines the phase difference between element pairs, such that the response pattern will favor the angle of incidence: For a uniformly excited, equally spaced linear array, it is convenient to define a variable  $\phi$  that contains all the phase information relevant to the array geometry:

$$\phi = (2\pi d/\lambda)\sin(\theta) + \alpha \quad (2)$$

where

- d spacing between successive elements,
- $\alpha$  phase shift between currents in the elements,
- $\lambda$  wavelength of excitation,
- $\theta$  polar angle measured from the normal to the array.

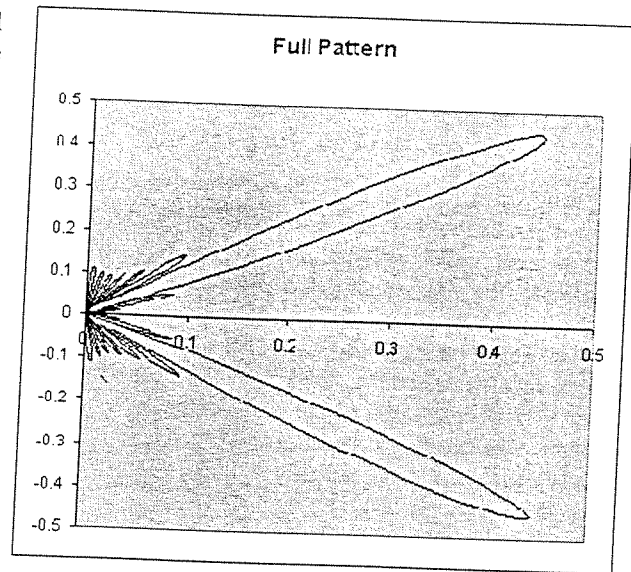


Figure 4. Response of 10 dipole antennas spaced one wavelength apart to a plane wave incident at 45°. The full pattern is symmetric about the horizontal axis, yielding a cone pattern similar to that observed in Figure 5.

The normalized array factor  $F_{\text{array}}$  for a linear array can then be written in terms of  $\varphi$  as

$$F_{\text{array}}(\varphi) = \sin(N\varphi/2)/N\sin(\varphi/2), \quad (3)$$

where  $N$  is the number of elements in the array. This equation has a number of important characteristics:

- Every maximum of  $F$  corresponds to constructive interference. Because  $F_{\text{array}}(\varphi)$  is periodic in  $N\varphi$  and  $\varphi$  is bound by  $2\pi d/\lambda$ , the total number of maxima (lobes) for the array will be  $(N-1)d/\lambda$ . Furthermore, if  $d/\lambda > 1$ , there will be more than one main lobe.
- $F_{\text{array}}(\varphi)$  always has maximum for  $\varphi = 0$ . Therefore, if we define  $\theta_0$  as the angle that produces the maximum intensity, then the current phase shift  $\alpha$  is given by

$$\alpha = -(2\pi d/\lambda)\sin(\theta_0) \quad (4)$$

By reciprocity, a plane wave incident on the array at angle  $\theta_0$  with wavelength  $\lambda$  will induce currents in the array such that a main lobe will open at  $2\theta_0$ . The simple linear array described above demonstrates a well-known property of antenna arrays: controlling the phase allows one to electronically steer the main beam and vice versa. This is called *main beam scanning*. We obtain the full pattern of the linear array by multiplying (1) and (3). The resulting pattern for a 10-element dipole array is shown in Figure 4. In the figure, this pattern is symmetric about the horizontal axis, the axis of the array.

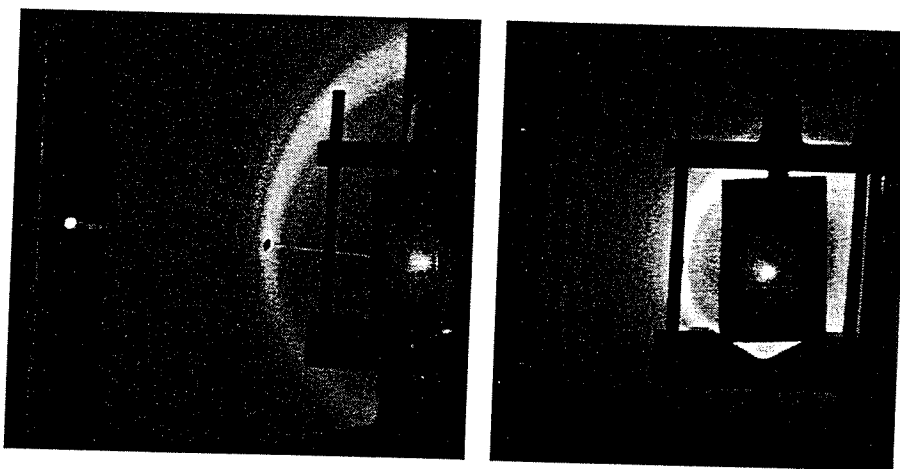


Figure 5. The two images above show the radiation patterns of the same sample of multi-walled carbon nanotubes grown vertically on a glass substrate. The screen was oriented almost parallel to the sample surface. For both frequencies, the main lobe opens along the paths of the incident and reflected beams. The bright spot in the center of the sample is the result of scattering off the sample surface and does not indicate the incident angle. Rather, the incident beam enters from beyond the right edge of the screen. The reflected beam passes through a hole to reduce the effect of scattering off the screen during the long (~10 sec) exposure.

The radiation pattern emitted by a random array of MWCNTs was produced experimentally for comparison to the theoretical curve shown in Figure 4. The experimental pattern is shown in Figure 5. The sample was mounted on a rotating platform, such that the direction normal to the sample surface could rotate through a plane formed by the incident and reflected beam. We then reflected laser light off the surface of the sample, placing a screen in the path of the reflected beam. A hole was made in the screen through which the spectral component of the reflected beam could pass, thus facilitating observation of the scattered component. In this configuration, the sample produced bright concentric rings on the screen, the brightest of which was bound by twice the angle of incidence and was symmetric about the normal to the array. The number of rings depended on the angle of incidence, but multiple rings were observed for any angle. The left and right images in Figure 5 were taken with a digital camera, showing these rings for green and red wavelengths, respectively.

The radiation pattern exhibited by our random planar array was surprisingly similar to the theoretical pattern for a linear array of equally spaced dipoles: they both produce concentric diffraction rings on a screen and the main lobe opens toward the angle of incidence. Using the principle of pattern multiplication, a phased planar array is simply an array of

linear arrays when the phase is unidirectional. Thus, one would expect a 2-D phased array to exhibit main beam scanning. However, there is one important difference. In the case of our planar array the axis of pattern symmetry was perpendicular to the plane of the array whereas a linear array has a symmetry axis along the array. While we have yet to explain the mechanism for this symmetry, we should note that the normal is the only unique axis for a random planar array. Further investigation is required to fully interpret these results.

### 2.3 Bandgap observations

Several experiments were conducted using unpolarized white light in an attempt to observe bandgap behavior in periodic arrays of aligned MWCNTs.

A bifurcated fiber was used to provide a white light source to a periodic MWCNT array. The bifurcated fiber consists of two optical fibers: a white light source fiber surrounded by a series of collector fibers that gather light returned directly back toward the source fiber. The light returned to the collector fibers was then detected by an Ocean Optics spectrometer. In addition, a 600 micron collector fiber was positioned to collect light reflected off the surface of the MWCNT array where

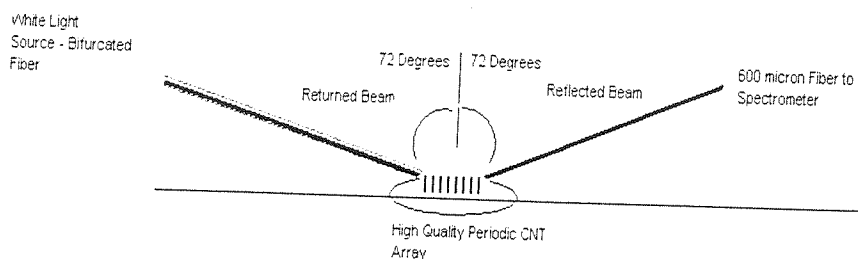


Figure 6. Experimental setup to evaluate the effect of white light interacting with the periodic MWCNT array.

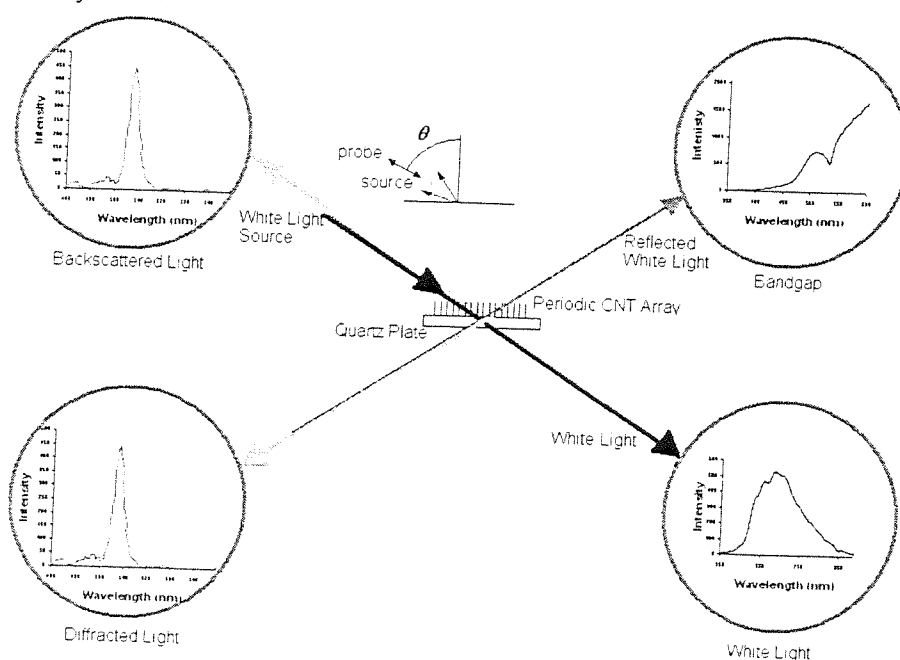


Figure 7. Unpolarized white light from the source interacts with a periodic MWCNT array. The p-polarized portion of the white light interacts with the nanotubes sending a diffraction pattern back to the white light source. A portion of the s-polarized is scattered by the quartz plate and the resulting p-polarized light then re-interacts with the nanotubes in the reflected beam sending a green diffraction pattern back in the direction of the reflected light as shown in the lower left corner. The remaining white light is transmitted through the sample as shown in the lower right corner and the reflected beam shown in the upper right hand corner now shows the bandgap associated with the periodic array of nanotubes.

the angle of incidence = the angle of reflectance as shown in Figure 6. Studies were conducted with the source light at  $72^\circ$  relative to the surface of the periodic MWCNT array. The angle of the bifurcated fiber and the angle of the 600 nanometer collector fiber were always the same relative to the MWCNT array as shown in Figure 6.

It was expected that the intensity of the band gap would be a function of the number of nanotubes that interacted with the light, as well as the length of the nanotubes. Our intent was to observe an absolute, polarization independent bandgap. Therefore, we used a randomly polarized white light source. It was found, however, that for this sample, *p*-polarized light interacted with the MWCNTs to a greater degree than did *s*-polarized light (see Figure 9). As a result, most of the incident *s*-polarized white light was simply reflected off the surface and detected by the detecting optical fiber, and the bandgap was found to be quite weak. It was noted during this experiment, that a narrow wavelength band of green light, similar in wavelength to the observed, weak bandgap, was returned directly toward the white light source.

A second experiment was conducted using a periodic MWCNT array that was grown on a quartz substrate. In this case, the reflected *s*-polarized component of the white light was scattered to a greater degree than with the silicon substrate sample, and the reflected beam contained relatively more *p*-polarized component. It was also found that the *p*-polarized light produced a green beam at a reflected angle as if mirrored from the surface normal. This is shown in Figure 7 as diffracted light.

Since a large majority of the white light was now interacting with the carbon nanotubes or being transmitted straight through the quartz substrate, the reflected light clearly showed the bandgap associated with the periodic MWCNT array (Figure 8).

The bandgap was also studied for its dependence on the angle of incidence of the white light source. The experiments were conducted by evaluating the reflected beam spectrum at several angles using the experimental setup as shown in Figure 6. The angle of incident was varied from  $85^\circ$  to  $70^\circ$  where  $85^\circ$  is near grazing angle for the white light upon the MWCNT array. The Ocean Optics spectrometer was operated in the reflectance mode and was corrected for background and dark current. The results of this experiment are shown in Figure 8.

Periodic MWCNT arrays were evaluated for their response to polarized light. A white light source equipped with a polarizer was used to evaluate the samples. The collector fiber was also equipped with a polarizer. The interaction was measured by directing the *p*-polarized light onto the sample and

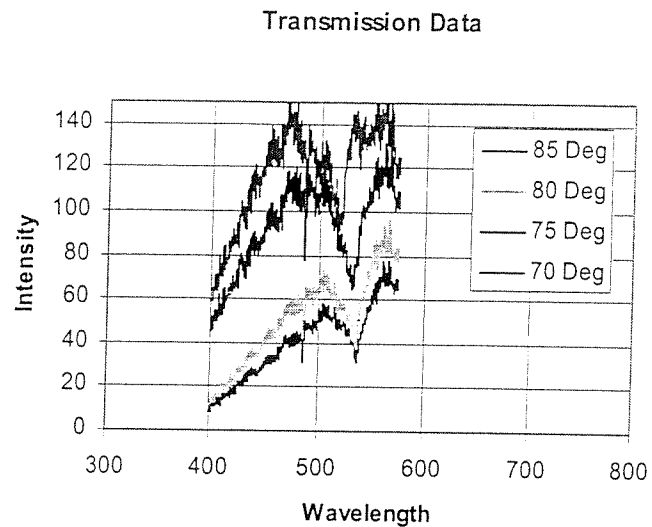


Figure 8. The effect of variations in angle of incident of the white light on the wavelength of the bandgap.

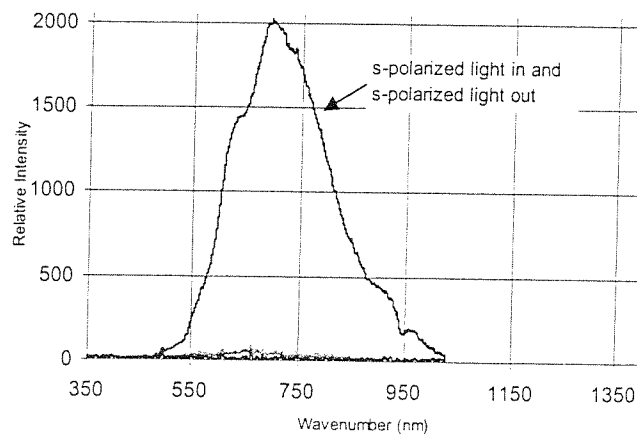


Figure 9. The periodic MWCNT array interacts with *p*-polarized light very strongly as shown by the reflected beam spectrum. *S*-polarized may also be scattered by the substrate on which the nanotubes are mounted producing a net interaction approaching 75%.

measuring the level of p-polarized light in the reflected beam. The experiments were repeated with s-polarized light. The experimental configuration is shown in Figure 6. The results of these experiments are shown in Figure 9.

### 3. SUMMARY

We have studied the optical properties of aligned, periodic and non-periodic MWCNT arrays. Our observations with regards to the non-periodic arrays are consistent with the light antenna hypothesis – that the MWCNTs are essentially a phased array of dipole light antennas, behaving in a manner that is similar to the way in which radio waves interact with radio antennas. This is evidenced in our previous work and again in the observation of main beam scanning and side lobe phenomena, detailed in this paper.

We have also presented preliminary experimental data regarding observed bandgap behavior in periodic MWCNT arrays. Though the results are encouraging, further work is required on the theoretical end, to make a convincing argument for the existence of such phenomena.

In general, our results indicate that it is possible to create optical surfaces comprised of aligned nanotubes that interact with light in a highly efficient and highly directional manner. The challenge is to incorporate the structured surfaces into conventional electronics. This would allow for the realization of a new class of electro-optic devices that could have a multitude of applications including highly efficient solar energy conversion, optical computing, UV/VIS/NIR detectors and imaging devices.

### REFERENCES

1. Hecht, E., Optics, 2<sup>nd</sup> Edition, Addison-Wesley, Reading, MA, 1987, pp. 281-282.
2. These calculations use the Numerical Electromagnetics Code, NEC-4 1D, authored by G. Burke et al, Lawrence Livermore National Laboratory
3. K. Kempa, B. Kimball, J. Rybczynski, Z. P. Huang, P.F. Wu, D. Steeves, M. Sennett, M. Giersig, D.V.G.L. Rao, D.L. Carnahan, D.Z. Wang, J.Y. Lao, W.Z. Li and Z. F. Ren, "Photonic Crystals Based on Periodic Arrays of Aligned Carbon Nanotubes", *NanoLetters* **3**, 13 – 18 (2003).
4. Z. P. Huang, D. L. Carnahan, J. Rybczynski, M. Giersig, M. Sennett, D. Z. Wang, J. G. Wen, K. Kempa, Z. F. Ren, "Growth of Large Periodic Arrays of Carbon Nanotubes", *Appl. Phys. Lett.* **82**, 460 – 462 (2003).
5. S. H. Jo, Y. Tu, Z. P. Huang, D. L. Carnahan, D. Z. Wang, Z. F. Ren, "Effect of length and spacing of vertically aligned carbon nanotubes on field emission properties", *Appl. Phys. Lett.* **82**, 3520 – 3522 (2003)
6. Y. Tu, Yuehe Lin, Z.F. Ren, "Nanoelectrode Arrays Based on Low Site Density Aligned Carbon Nanotubes", *NanoLetters*, **3**, 107 – 109 (2003).
7. Pengfei Wu, B. Kimball, J. Carlson and D. V. G. L. N. Rao, *Phys. Rev. Lett.* **93**, (2004).
8. B. Kimball, J. Carlson, K. Kempa, W. Li, Z. Ren, P. Wu, D.V.G.L.N. Rao, J. Rybczynski, M. Giersig, Z. Huang, D. Carnahan, D. Steeves, M. Sennett, SPIE Proc. Vol. 5224, August 2003.
9. Y. Wang, K. Kempa, B. Kimball, J. B. Carlson, G. Benham, W. Z. Li, T. Kempa, J. Rybczynski, A. Herczynski, and Z. F. Ren, "Receiving and transmitting light-like radio waves: Antenna effect in arrays of aligned carbon nanotubes" *Appl. Phys. Lett.* **85**, 2607 – 2609 (2004).
10. Brian Kimball, Joel B. Carlson, Diane Steeves, Krzysztof Kempa, Zhifeng Ren, Pengfei Wu, Thomas Kempa, Glynda Benham, Y. Wang, Wenzhi Li, A. Herczynski, Jacob Rybczynski and D.G.V.L.N. Rao, "Diffraction effects in honeycomb arrays of multiwalled carbon nanotubes", SPIE Proc. Vol. 5515, Aug 2004.
11. Steeves, D., Kimball, B. R., "Nonlinear Transmission and Scattering of Multiwalled Carbon Nanotubes Suspended in an Index Matched Solid Matrix and Optical Dye Solution", SPIE Proc. Vol. 4797, July 2002.
12. Cassagne, D.; Jouanin, C.; Bertho, D. *Phys. Rev. B* **53**, 7134 (1996).
13. Y. Wang, J. Rybczynski, D. Z. Wang, K. Kempa, Z. F. Ren, W. Z. Li, and B. Kimball, "Periodicity and alignment of large-scale carbon nanotubes arrays" *Appl. Phys. Lett.* **85**, 4741 – 4743 (2004).
14. W. Stutzman and G. Thiele, Antenna Theory and Design, New York: John Wiley & Sons, 1981.